Chapter 6

Selective transport of sphingolipids from the sub-apical compartment to the apical plasma membrane via rab11-positive intermediate compartments

Sven C.D. van IJzendoorn, Margriet Jonker and Dick Hoekstra

Abstract

The sub-apical compartment (SAC) constitutes an intrinsic part of the transcytotic pathway and plays an important role in the polarized sorting of proteins and lipids. In a previous study, we have shown that in the SAC fluorescent sphingolipid analogs are sorted. Thus, from the SAC, C_6-NBD-glucosylceramide (GlcCer) is targeted to the apical plasma membrane (PM), while C_6-NBD-galactosylceramide (GalCer) and -sphingomyelin (SM) are targeted to the basolateral PM (van IJzendoorn, S.C.D. and Hoekstra, D. 1998. *Journal of Cell Biology* 142, 683-696). In addition, SAC-associated SM can be rerouted to the apical surface when the cells are treated with dibutyryl cAMP (chapter 4). Interestingly, it was shown that the signal-regulated SAC-to-apical transport of SM was via a distinct pathway than that followed by GlcCer. In this study, evidence is provided that suggests that two distinct pathways from the SAC to the apical PM exist, a direct route and a route that involves rab11-containing sub-apical intermediate compartments, and that (cAMP-) regulated SAC-to-apical targeting of SM is specifically via the rab11-mediated pathway. These data suggest that regulated polarized transport from the SAC is closely related to a subcompartmental organization of the SAC.

Introduction

Polarized cells have distinct plasma membrane (PM) domains, an apical and a basolateral domain (Simons and Fuller, 1985). Each domain is characterized by a specific composition of proteins and lipids that allow the cell to exert its specific functions at the different extracellular environments. To establish and maintain such membrane compositions, intracellular machineries are operational that sort and transport proteins and lipids to the correct surface. The generation of different PM domains and the endogenous expression of (at least some) polarity markers are dissociable events, which is reflected by the observation that many domain-specific proteins show similar expression patterns in both the nonpolarized and polarized form of differentiating cells (Bender et al., 1998; Krämer et al., 1997). Hence, when cells acquire a polarized phenotype, the need for redistribution of PM components seems evident. In addition, also in fully polarized cells, the localization of PM proteins may be switched from apical to basolateral, or vice versa, by the action of extracellular signals, emphasizing the plasticity of cell polarity (Schwartz et al., 1985) and, consequently, of polarized sorting and targeting. Redistribution of PM components by definition involves transcytosis, a process that for many proteins and lipids largely bypasses the trans-Golgi network (Futter et al., 1998; van IJzendoorn et al., 1997), where sorting in the biosynthetic route is believed to be orchestrated (Traub and Kornfeld, 1997). The SAC constitutes an intrinsic part of the transcytotic pathways where it connects the apical and basolateral endocytic routes. Indeed, both transcytosing and recycling proteins and lipids have been reported to pass through the SAC (Apodaca et al., 1994; Futter et al., 1998; van IJzendoorn and Hoekstra, 1998; Zacchi et al., 1998). In this compartment, well-known sorting machineries, including those involving clathrin-adaptin complexes (Futter et al., 1998; Okamoto et al., 1998) are harbored. Also sorting of fluorescent (C_6-NBD) sphingolipid analogs has recently been demonstrated to occur in the SAC. Thus, whereas C_6-NBD-sphingomyelin (SM) and –galactosylceramide (GalCer) are rapidly transported from the SAC to the basolateral surface, C_6-NBD-glucosylceramide (GlcCer) is efficiently transported to the

apical PM domain (van IJzendoorn and Hoekstra, 1998). Given its central position in the different transport routes where apical and basolateral constituents mix, and the presence of different sorting machineries, it is therefore attractive to propose a crucial involvement of the SAC in the polarized disposition of proteins and lipids. However, the regulation of sorting and polarized traffic from the SAC remains largely obscure.

Three small GTPases, rab11 (Casanova et al., 1998), the epithelium-specific rab17 (Zacchi et al., 1998; Hunziker and Peters, 1998), and rab25 (Casanova et al., 1998) have been proposed to play a role in polarized trafficking from the SAC. Intriguingly, whereas all three rabs localize to the SAC, their localization often does not completely overlap, as judged by indirect immunofluorescence analysis. Moreover, whereas the SAC, as judged by the redistribution of rab11 and rab25, appears to depend on intact microtubules for its spatial organization (Casanova et al., 1998), the SAC as marked by rab17 is not (Zacchi et al., 1998). These data raise intriguing questions as to the possibility of subcompartmentalization of the SAC (van IJzendoorn and Hoekstra, 1999). Thus, it is tempting to suggest that different rab proteins act at specific SAC subcompartments, where they regulate the transfer of molecules to, from and/or between these compartments.

In addition to rab proteins, different protein kinases have been shown to modulate transport from the SAC (Hansen and Casanova, 1994; Cardone et al., 1994) and, moreover, interfere with cell polarity (Zegers and Hoekstra, 1997). In MDCK cells, transcytosis of the polymeric Ig receptor (pIgR) from the SAC to the apical surface is stimulated when it has bound IgA (Luton et al., 1998). Binding of IgA to the pIgR was also reported to induce translocation of protein kinase C, which, in turn, stimulates the trafficking of transcytosing and recycling IgA-pIgR complexes from the SAC to the apical PM (Cardone et al., 1994). Increased levels of cAMP were shown to inhibit apical to basolateral transcytosis of C_6-NBD-SM and caused the apical rerouting of the lipid in polarized HepG2 cells (van IJzendoorn et al., 1997). Concomitantly, in the presence of cAMP an enhanced apical PM biogenesis occurred (Zegers and Hoekstra, 1997; van IJzendoorn and Hoekstra, submitted). Detailed microscopical analysis revealed a protein kinase A (PKA)-mediated basolateral to apical switch of C_6-NBD-SM targeting from the SAC. Moreover, in cAMP-stimulated cells, SAC-to-apical transport of C_6-NBD-SM and C_6-NBD-GlcCer could be distinguished by calmodulin antagonists which specifically inhibited trafficking of the SM analogue from the SAC (van IJzendoorn and Hoekstra, manuscript submitted). Interestingly, activation of PKA stimulated basolateral to apical transcytosis of pIgR, presumably at the level of the SAC. However, stimulation of PKA did not affect the apical recycling of re-internalized pIgR-IgA complexes (Hansen and Casanova, 1994). Together, these data thus suggests the existence of distinct pathways that lead from the SAC to the apical PM, which may be differentially employed under conditions of (cAMP-) stimulated apical targeting.

In this study, evidence is provided that suggests that in cAMP-stimulated HepG2 cells, C_6-NBD-SM is targeted from the SAC to the apical PM via distinct, rab11-positive intermediate compartments. In contrast, SAC-to-apical transport of C_6-NBD-GlcCer bypassed the rab11-positive compartments. We propose that two distinct pathways from the SAC to the

apical PM exist, a direct route and a route that involves rab11-positive intermediate compartments, and that (cAMP-) regulated apical targeting specifically employs the rab11-mediated pathway. The results suggest a close relation between regulated polarized transport from the SAC and a subcompartmental organization of the SAC.

Materials and Methods

Affinity purified rabbit anti-rab11 antibody was a generous gift from Dr. D. Sabatini, New York University School of Medicine, New York, USA. The monoclonal anti-β-tubulin antibody was purchased from Sigma Chemical Co., St. Louis, MO/USA. FITC- and Cy3-conjugated secondary antibodies were from Nordic Immunologic Laboratories, Tilburg/The Netherlands and Jackson Immunoresearch Laboratories, Inc, West Grove, PA/USA, respectively. Sphingosylphosphorylcholine and 1-ß-glucosylsphingosine were from Sigma Chemical Co., St. Louis, MO/USA. Albumin (from bovine serum, fraction V) was bought from Fluka Chemie AG, Buchs/Switzerland. 6-[*N*-(7-nitrobenz-2-oxa-1,3-diazol-4-yl)amino]hexanoic acid (C_6-NBD) was obtained from Molecular Probes, Eugene, OR/USA. DMEM was purchased from GIBCO BRL (Life Technologies), Paisley/Scotland. Fetal calf serum (FCS) was bought from BioWhittaker, Verviers/Belgium. Paraformaldehyde and sodiumdithionite ($Na_2S_2O_4$) were from Merck, Darmstadt/Germany. Dibutyryl cyclic AMP (dbcAMP) and nocodazole were obtained from Boehringer Mannheim, Mannheim/Germany. All other chemicals were of analytical grade.

Cell Culture
HepG2 cells were cultured as described elsewhere (van IJzendoorn and Hoekstra, 1998). For experiments, cells were plated onto ethanol-sterilized glass coverslips. Cells were used three days after plating. At that time the cells had reached an optimal ratio of polarity versus density, i.e. number of BC versus number of cells (van IJzendoorn et al., 1997).

Indirect Immunofluorescence Studies
Cells were washed with HBSS, fixated with 4% paraformaldehyde at RT for 20 min, and washed twice with HBSS. Permeabilization was performed by incubating in HBSS, supplemented with 5% FCS and 0.1% Triton X-100, at 37°C for 15 min. Cells were then washed three times with HBBS/2.5% FCS and incubated in HBBS/5% FCS at 37°C for 1 h to block nonspecific binding sites. After washing three times with HBBS/2.5% FCS, cells were incubated with anti-rab11 or anti-β-tubulin antibody, diluted in HBSS/2.5% FCS, at 37°C for 2 h. Cells were then washed three times with HBSS/2.5% FCS and incubated with the appropriate Cy3- or FITC-conjugated secondary antibody, diluted in HBSS/2.5% FCS, at 37°C for 45 min. To prevent bleaching, cells were embedded in glycerol containing 2.5% 1,4-diazobicyclo [2.2.2.]octane prior to microscopical examination.

Synthesis of C_6-NBD-Labeled Sphingolipids
C_6-NBD-GlcCer and C_6-NBD-SM were synthesized from C_6-NBD and 1-ß-glucosylsphingosine and Sphingosylphosphorylcholine, respectively, as described elsewhere (Kishimoto, 1975; Babia et al., 1994). The C_6-NBD-lipids were stored at -20°C and routinely checked for purity.

Labeling Cells with C_6-NBD-Lipids
Cells were washed three times with HBBS. C_6-NBD-GlcCer or C_6-NBD-SM was dried under nitrogen, redissolved in absolute ethanol and injected into HBSS under vigorous vortexing. The final concentration of ethanol did not exceed 0.5% (v/v). All lipid analogs were administered to the cells at a concentration of 4 μM.

Transport of C_6-NBD-Lipids from the SAC
In order to monitor SAC-associated sphingolipid transport, the SAC were first preloaded with lipid analogue as

described elsewhere (van IJzendoorn and Hoekstra, 1998). In brief, cells were washed with HBBS and incubated with C_6-NBD-SM or -GlcCer at 37°C for 30 min to allow internalization of the lipid analogue from the basolateral surface followed by transcytosis (Zegers et al., 1997; Zegers and Hoekstra, 1998, van IJzendoorn et al., 1997, van IJzendoorn and Hoekstra, 1998). The remaining basolateral pool of lipid analogue was then depleted by a back exchange procedure (5% BSA (w/v) in HBSS, pH 7.4 at 4°C for 2 x 30 min). Then, lipid analogue was chased from the apical, bile canalicular PM into the SAC by an incubation at 18°C for 60 min in back exchange medium. Finally, NBD-fluorescence remaining at the luminal leaflet of the apical PM was abolished by incubating the cells with 30 mM sodiumdithionite (diluted from an 1 M stock solution in 1 M Tris buffer, pH 10). After these incubation steps, the majority of the lipid analogue was associated with the SAC (see Results; cf. van IJzendoorn and Hoekstra, 1998). In some experiments, cells were subsequently treated with 33 μM nocodazole, 100 μM dibutyryl cAMP (dbcAMP) or both, at 4°C for 30 min. Transport of the lipid analogs from the SAC was monitored by incubation at 37°C in back exchange medium. When required, nocodazole, dbcAMP or both were kept present during the transport assay.

In order to quantitate transport of the lipid analogs to and from the apical, bile canalicular (BC) membranes, the percentage of NBD-positive BC membranes was determined as described elsewhere (van IJzendoorn et al., 1997; van IJzendoorn and Hoekstra, 1998). Briefly, BC were first identified by phase contrast illumination, and then classified as NBD-positive or NBD-negative under epifluorescence illumination. Distinct pools of fluorescence were discerned, present in vesicular structures adjacent to BC, which are defined as sub-apical compartments (SAC, cf. van IJzendoorn and Hoekstra, 1998). Together, BC and the SAC thus constitute the bile canalicular, apical pole (BCP) in HepG2 cells. Therefore, within the BCP region the localization of the fluorescent lipid analogs will be defined as being derived from BC, the SAC, or both. At least 50 BCP per coverslip were analyzed. Data are expressed as the mean ± SEM of at least two independent experiments, carried out in duplicate.

Results

Localization of Rab11 in Polarized and Nonpolarized HepG2 Cells

HepG2 cells progressively acquire a polarized phenotype after plating, which is characterized by the formation of intercellular microvilli-lined vacuoles that represent the apical, bile canalicular plasma membrane (BC) domain in hepatic cells. Three days after plating, the cells have reached maximum polarity, i.e. in terms of number of BC per number of cells (van IJzendoorn et al., 1997). In the experiments described in this study, typically ~ 40% of the cells are polarized in a 3 d-old cell culture (our unpublished observations). In order to examine the intracellular localization of endogenous rab11 in HepG2 cells, cells were fixed with 4% paraformaldehyde and processed for indirect immunfluorescence microscopy as described in Materials and Methods. Rab11 was found exclusively localized in sub-apical compartments, which are seen as a belt that closely surrounds the apical, bile canalicular plasma membrane (Fig. 1a, b). Interestingly, endogenous rab11 also showed immunoreactivity in nonpolarized HepG2 cells. In these cells, rab11 was confined to the juxtanuclear region (Fig. 1c, d), consistent with its localization in fibroblasts (Ren et al., 1998; Ullrich et al., 1996). Hence, endogenous rab11 is present in both polarized and non-polarized HepG2 cells, but localizes to distinct sites.

Sub-apical compartments have been proposed to be analogous to the recycling endosomes in non-polarized cells (reviewed in van IJzendoorn and Hoekstra, 1999). Both the sub-apical compartments in polarized cells and recycling endosomes in nonpolarized cells are concentrated around the microtubule-organizing center. In order to compare the localization

of the rab11-positive structures with that of the microtubule-organizing center in nonpolarized and polarized HepG2 cells, the following experiment was performed. First, the microtubule network was destroyed by incubating the cells with 33 µM nocodazole (Fig. 2a, b). Then, nocodazole was removed and the cells were further incubated in HBSS at 37°C. After different times of incubation, cells were fixed and processed for indirect immunofluorescent staining of tubulin (see Materials and Methods). As shown in figure 2c and d, 45 min after removal of the nocodazole, a bright fluorescent punctuate staining was observed just next to the apical PM domain in polarized cells, and in the juxtanuclear region in nonpolarized cells.
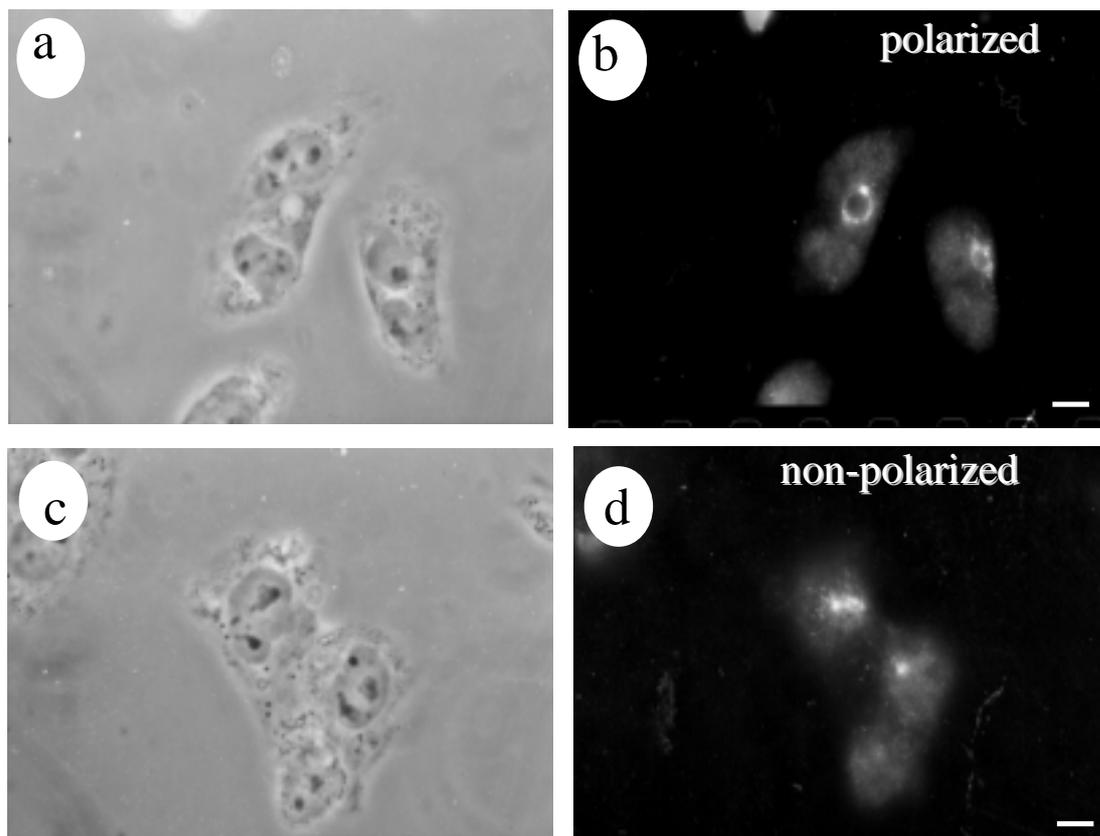

Figure 1. Rab11 localizes to sub-apical and juxtanuclear compartments in polarized and non-polarized HepG2 cells, respectively. Cells were fixated and endogenous rab11 was visualized by indirect immuno-fluorescence microscopy as described in Materials and Methods. In b and d, immunoreactivity with anti-rab11 antibody in polarized and non-polarized HepG2 cells, respectively, is shown. Note that a clear labeling of rab11 was also observed in the lower cell in d but in another plane of focus. A and c are phase contrast images to b and d, respectively.

These punctuate spots are likely to represent the microtubule-organizing center, as evidenced by the progressive growth of microtubules from these spots, observed 180 min after removal

of the nocodazole (Fig. 2e and f). Thus, the apparent localization of the rab11-positive structures in the direct vicinity of the microtubule-organizing center in both nonpolarized and polarized HepG2 cells supports the proposed analogy between the sub-apical compartments and the recycling endosomes.

The Spatial Organization of the Rab11-Positive Compartments is Dependent on Intact Microtubules

The similarity in localization of the rab11-positive compartments and the microtubule-organizing center prompted us to investigate whether the spatial organization of these compartments was dependent on microtubules, as has been proposed before in polarized MDCK cells (Casanova et al., 1998). To this end, cells were treated with nocodazole and subsequently stained for rab11 as described in Materials and Methods. As shown in figure 3b, profound labeling of rab11 in sub-apical structures, as well as those in the juxtanuclear region in non-treated cells (Fig. 1 and Fig. 3a), was no longer observed. Instead, specific punctate labeling was observed throughout the cytoplasm, suggesting that the organization of the rab11-positive structures is microtubule-dependent.

We next examined whether the original organization of the rab11-positive compartments could be reconstituted following a recovery from the nocodazole. Thus, after treatment with nocodazole, cells were washed three times with HBSS and further incubated in HBSS at 37°C. As shown in figure 3c, large fluorescently labeled structures appeared in the cytoplasm and along the lateral membranes, where it organized into patch-like structures (arrows). Three hours after removal of the nocodazole, rab11 could still be observed along the lateral membranes (Fig. 3d), albeit to a much lesser extent. Moreover, the profound sub-apical rab11 staining was recovered, similar in appearance as seen in non-treated cells (Fig. 3a).

The Structural Organization of the Sub-Apical Compartment where Sphingolipids are Sorted is Not Dependent on Microtubules

Apically endocytosed C_6-NBD-SM and -GlcCer have also been reported to accumulate in sub-apical compartments, SAC, at 18°C. It was demonstrated that in the SAC, sorting of C_6-NBD-SM and –GlcCer occurs. Thus, C_6-NBD-SM is rapidly transported from the SAC to the basolateral domain, whereas the GlcCer analogue is efficiently targeted back to the apical PM (van IJzendoorn and Hoekstra, 1998). In order to investigate the requirement for intact microtubules for the organization of C_6-NBD-sphingolipid-labeled SAC, the SAC were loaded with C_6-NBD-SM as described in Materials and Methods. The cells were then treated with 33 µM nocodazole or HBSS (control) at 4°C for 30 min. Nocodazole effectively destroys the microtubule network (Fig. 2b, cf. Zegers et al., 1998). However, as shown in figure 4a-d, nocodazole did not affect the organization of the C_6-NBD-SM-labeled sub-apical compartments. Similar results were obtained for C_6-NBD-GlcCer-labeled SAC (data not shown), which is entirely consistent with our previous observations (van IJzendoorn and
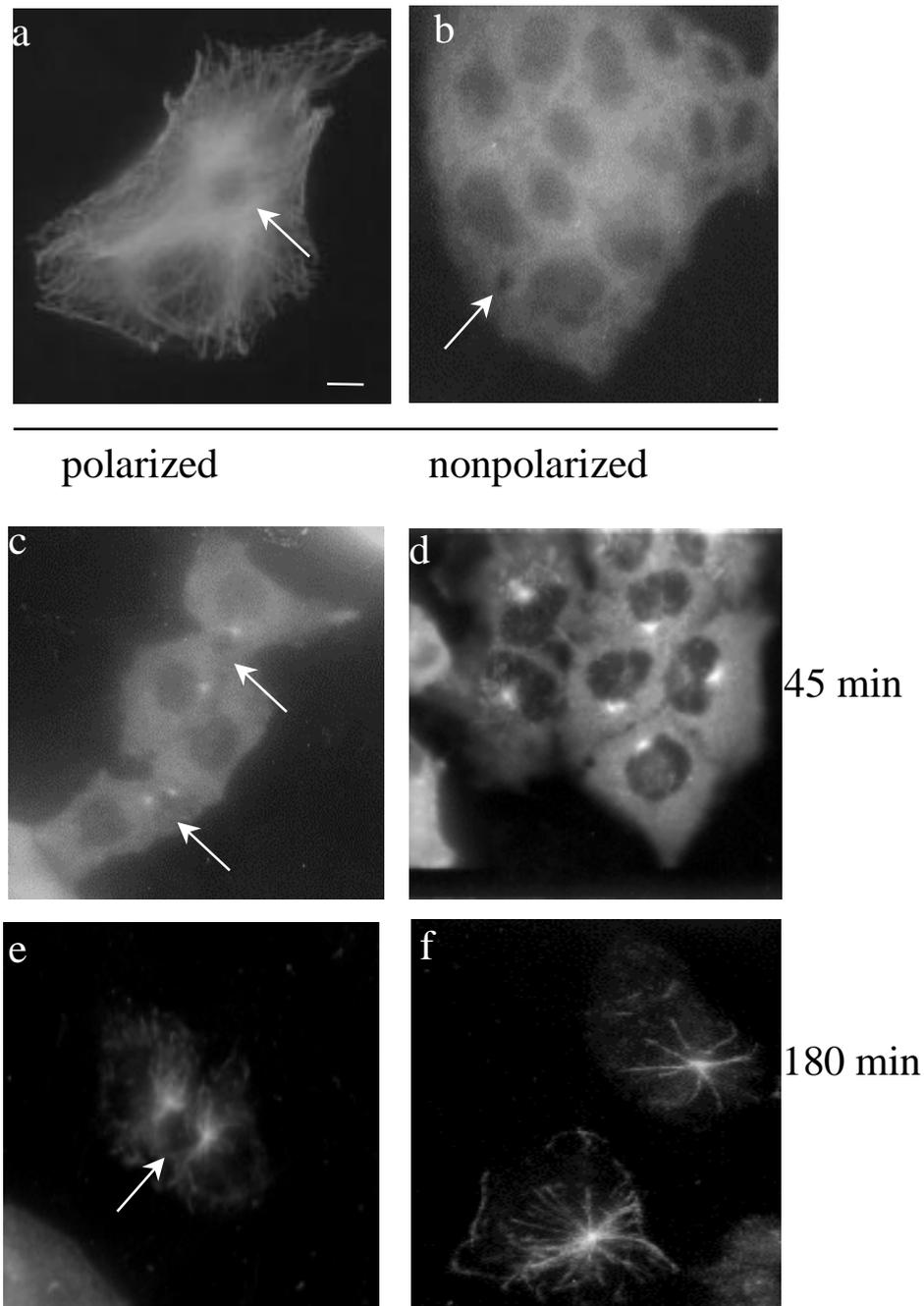
Figure 2. The MTOC in polarized and non-polarized HepG2 cells. In a, the microtubule network in polarized cells is shown, using an anti-β-tubulin antibody. In b, cells were treated with nocodazole at 4°C for 30 min, which disrupts the microtubule network. Note that the fine structures as observed have completely disappeared. Cells were sub-sequently washed and allowed to recover from the nocodazole for 45 (c and d) or 180 (e and f) min, and stained for β-tubulin. Note the appearance of sub-apical and juxta-nuclear punctate labeling in polarized (c and e) and non-polarized (d and f) cells, respectively, which represents the MTOC, as evidenced by the growth of microtubules from these spots (e and f). Arrows point to BC. Bar 5μM.

Hoekstra 1998). Hence, the data suggest that the SAC, in which the C_6-NBD-sphingolipids accumulate at 18°C, is distinct from the compartment that showed immunoreactivity with the anti-rab11 antibody (Figs. 1b and 3a).

Figure 3. The spatial organization of the rab11-postive com-partments is depen-dent on intact microtubules. In a, rab11 localization is shown and is pronounced in the sub-apical region (see also Fig. 1b). After treatment with nocodazole, the rab11-postive com-partments dispersed into the cytosol (b). After removal of the nocodazole by washing, and incu-bating the cells at 37°C for 75 min in HBSS, rab11- posi-tive structures re-organized into larger structures (arrows) throughout the cyto-sol and along the lateral PM (c). Note that no significant sub-apical enrichment was observed at this time. Following a recovery for 180 min, the large vesicular structures in the cytosol and along the lateral PM (arrows) had disappeared and a profound labeling subjacent to the apical PM domain was apparent (d). C1, C2, etc. mark the different cells. Asterisks mark the BC. Bar. 5 μM.
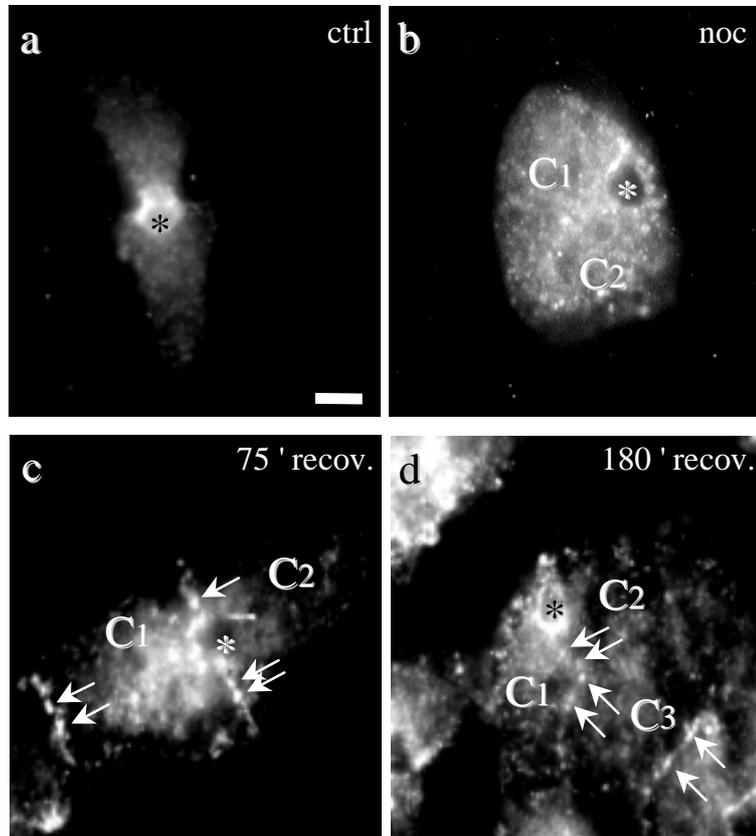
Transport of C_6-NBD-GlcCer from the SAC to the Apical PM Domain does Not Require Intact Microtubules

In order to examine the effect of nocodazole on transport of C_6-NBD-GlcCer from the SAC to the apical PM, the SAC were loaded with C_6-NBD-GlcCer and cells were subsequently treated with nocodazole or HBSS as described in the previous paragraph. In both control and nocodazole-treated cells, the percentage of labeled BCP remained constant at ~90% (Fig. 5a and c), suggesting that the GlcCer analogue recycled at the apical pole of the cells irrespective of the presence of nocodazole. Indeed, within the labeled BCP, C_6-NBD-GlcCer localized to the BC, the SAC or both, indicative for its apical recycling in both control and nocodazole-treated cells (Fig. 4i-l; Fig. 5b and d). Hence, the data suggest that transport of C_6-NBD-GlcCer from the SAC to the apical PM is microtubule-independent.
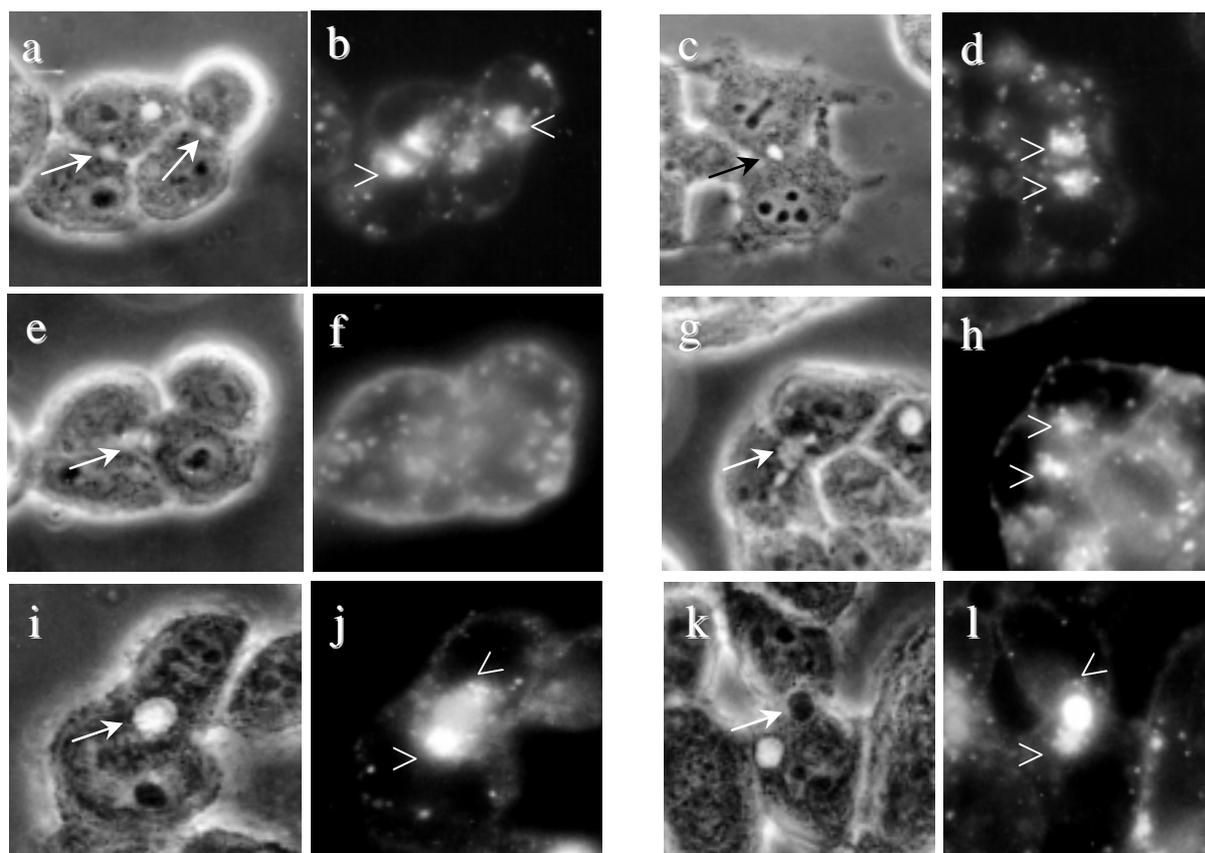
Figure 4. Effect of nocodazole on SAC-to-BC transport of C_6-NBD-sphingolipids. The SAC were loaded with either lipid analogue as described in Materials and Methods. In b and d, the sub-apical labeling pattern of C_6-NBD-SM (arrowheads) is shown in control (b) and nocodazole-treated (d) cells. A and c are the corresponding phase contrast micrographs, with arrows pointing to the BC. Note that the labeling pattern does not change after nocodazole treatment, indicating that the spatial organization of the SAC does not depend on intact microtubules. Identical results were obtained with C_6-NBD-GlcCer-loaded SAC (not shown).

Subsequently, the SAC-loaded cells were incubated for 20 min at 37°C in back exchange medium, with or without nocodazole. In the absence of nocodazole, SM disappeared from the SAC and the sub-apical region of the cell (f; e, corresponding phase contrast, arrow marks the BC), whereas in its presence the SAC, loaded with the SM analogue, remained prominently labeled (h, arrowheads; g, corresponding phase contrast. Arrow indicates BC). Note that nocodazole inhibits SAC-to-basolateral trafficking of SM. Panels j and l show the fate of SAC-loaded GlcCer, following the 20 min incubation period at 37°C in either the absence (j) or presence of nocodazole (l). The corresponding phase contrast images are presented in i and k; arrow mark the localization of BC. Note that in this case, the lipid analogue resided in the BCP area, labeling both SAC and BC (arrowheads). Bar. 5 µM.

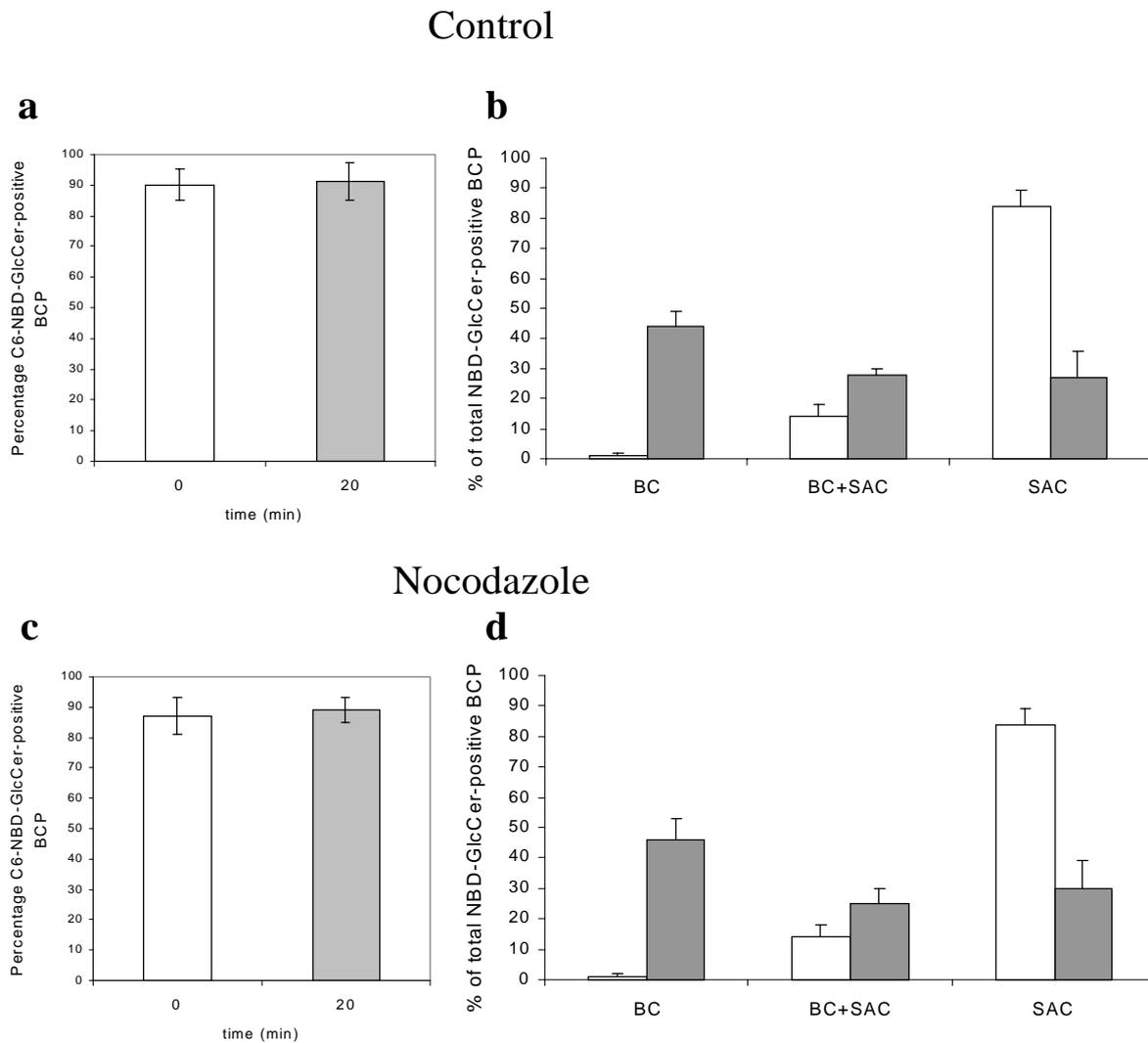## Control

a   **b**

Nocodazole

c   **d**

Figure 5. Nocodazole does not inhibit SAC-to-apical transport of C_6-NBD-GlcCer. SAC were loaded with C_6-NBD-GlcCer as described in Materials and Methods. Cells were treated with HBSS with or without nocodazole at 4°C for 30 min and incubated in back exchange medium, with or without nocodazole for 20 min. Figures a and b represent the BCP distribution in non-treated cells; c and d that in treated cells. In a and c, the percentage of C_6-NBD-GlcCer-labeled BCP is shown prior and after the chase (20 min 37°C). In b and d, the distribution of the lipid analogue within the BCP is specified (white bars: prior to the chase; gray bars: after the chase).

Transport of C_6-NBD-SM from the SAC to the basolateral PM Requires Intact Microtubules

The microtubule-dependence of C_6-NBD-SM transport from the SAC, in which the lipid analogue had been accumulated, was examined similarly as described for the GlcCer analogue in the foregoing paragraph. Following a 20 min chase at 37°C, the percentage of C_6-NBD-SM-labeling at the bile canalicular pole (BCP; see Materials and Methods) in control cells decreased from ~90 to ~55%, reflecting transport of the lipid analogue out of the apical pole (Fig. 6a). Indeed, analysis of the remaining fraction of the lipid analogue that still associated

with the BCP revealed, that most of the lipid analogue was in the SAC alone (Fig. 4e, f; Fig. 6b), suggesting that little if any C_6-NBD-SM was transported from the SAC to the apical PM (compare white and gray bars in Fig. 5b; cf. van IJzendoorn and Hoekstra, 1998). By contrast, in nocodazole-treated cells, the percentage of C_6-NBD-SM labeled BCP did not decrease, but remained constant at ~90% during the chase (Fig. 6c), indicating that nocodazole inhibited transport of the SM analogue out of the BCP. Analysis of the distribution of the SM analogue within the BCP revealed that C_6-NBD-SM nearly exclusively labeled the SAC while the labeling of BC was essentially negligible (Fig. 4g, h; Fig. 6d). Hence, the data suggest that nocodazole inhibits SAC-to-basolateral transport of C_6-NBD-SM, resulting in its entrapment in the SAC.

Transport of C_6-NBD-SM from the SAC to the Apical PM in Dibutyryl cAMP-Treated Cells is Via Rab11-Postive Compartments

Whereas in optimally polarized HepG2 cell cultures, i.e. 3 d after plating (van IJzendoorn and Hoekstra, 1998), C_6-NBD-SM is targeted from the SAC to the basolateral domain, a rerouting of the SM to the apical BC can be induced upon treatment of the cells with dbcAMP (van IJzendoorn et al., 1997). Recently, we have demonstrated that this rerouting of the lipid occurs in the SAC (van IJzendoorn and Hoekstra, submitted). In order to examine whether SAC-to-apical transport of C_6-NBD-SM in dbcAMP-treated cells required intact microtubules, apically derived C_6-NBD-SM was first chased into the SAC (see above). Cells were then incubated with 100 µM dbcAMP at 4°C for 30 min. Subsequently, transport from the SAC was triggered by raising the temperature to 37°C. The incubation was done in back exchange medium, supplemented with dbcAMP. As shown in figure 7a, the percentage of C_6-NBD-SM-labeled BCP remained unaltered during a 20 min chase from the SAC, which indicates a lack of transport to the basolateral domain of the cells, similarly as observed in nocodazole treated cells (Fig. 6c). However, whereas in nocodazole-treated cells C_6-NBD-SM remained associated with the SAC, in dbcAMP-treated cells, BCP-associated C_6-NBD-SM was redistributed to the apical PM. Thus, the lipid analogue labeled BC, the SAC, or both (Fig. 7b and Fig. 8a, b). Hence, in dbcAMP-treated cells, polarized transport of C_6-NBD-SM from the SAC is rerouted to the BC.

To examine the microtubule-dependence of SAC-to-BC transport of C_6-NBD-SM, nocodazole was included during the dbcAMP incubation step. Prior to the chase, 90% of the BCP was labeled with C_6-NBD-SM of which the vast majority labeled only the SAC (Fig. 7c and d, white bars). When the distribution of C_6-NBD-SM, was analyzed following the chase in the presence of dbcAMP and nocodazole, labeling was no longer exclusively confined to the apical pole of the cells, as observed in cells only treated with dbcAMP (Fig. 8a, b), but redistributed to the cytoplasm (Fig. 8 c, d). Accordingly, the percentage of C_6-NBD-SM-labeled BCP was dramatically decreased to ~55% (Fig. 7c, light gray bar). A major part of the remaining fraction of C_6-NBD-SM that was still associated with the BCP was located in the SAC only (Fig. 7d; light gray bars). Note that in the absence of nocodazole, the extent of BC labeling was approximately 2-fold higher than in its presence (light gray bars in Fig.7b and d).

The data thus suggest that nocodazole inhibited SAC-to-BC transport of C_6-NBD-SM, as induced by treatment of the cells with dbcAMP.

The decrease of the percentage C_6-NBD-SM-labeled BCP (Fig. 7c; white vs. light gray bar) would suggest transport of the SM analogue out of the apical pole, presumably towards the basolateral plasma membrane domain. However, nocodazole inhibited transport of C_6-NBD-SM from the SAC to the basolateral surface in control cells (Fig. 6c, d). Therefore, it is unlikely that the SM analogue which seemingly disappeared from the BCP, would have entered a basolateral directed pathway. Rather, a likely explanation for the apparent decrease in labeled BCP could be that the C_6-NBD-SM was in fact transported from the nocodazole-inert SAC to the drug-sensitive rab11-positive sub-apical compartments. Because of the dispersed organization of the latter compartments in nocodazole-treated cells (Fig. 3b, c), C_6-NBD-labeled structures will therefore not be recognized as being part of the transport pathway to the apical membrane and hence qualify as compartments belonging to the bile canalicular pole. Concomitant with the inhibited delivery of C_6-NBD-SM to the BC in nocodazole-treated cells (Fig. 7d), this might thus explain the apparent decrease in labeled BCP. To test this hypothesis, we therefore examined the fate of the lipid analogue, following recovery from the nocodazole-block. After the removal of nocodazole, microtubules start to re-grow from the microtubule-organizing center in a time-dependent manner (see Fig. 2). In addition, we have previously shown that a nocodazole-induced block of transport can be overcome after subsequent prolonged incubation in the absence of the compound (van IJzendoorn and Hoekstra, 1998). Hence, following the chase of C_6-NBD-SM from SAC in dbcAMP/nocodazole-treated cells, the cells were washed three times with HBSS and incubated for an additional 75 min in back exchange medium at 37°C in the absence of nocodazole. Fluorescence microscopic examination revealed that, upon recovery from the nocodazole block, the lipid analogue was redistributed again to the BC and SAC (Fig. 8e, f). Indeed, quantifying its redistribution after recovery, C_6-NBD-SM was found to label BCP region to a similar extent as that in non-treated cells, increasing from ~55 in the presence of the drug to ~ 85% upon recovery (Fig. 7). Importantly, since all incubations were performed in BSA-containing medium, thus preventing any re-internalization from the basolateral surface, the increase in the percentage C_6-NBD-SM-labeled BCP must have been due to 'recruitment' of lipid analogue from intracellular compartments that localize to the apical cytoplasm in the absence of nocodazole. Indeed, the amount of cell-associated NBD-fluorescence did not significantly decrease during the incubations, as evidenced by quantification of the C_6-NBD-SM extracted from the cells (data not shown). The data thus suggest that after recovery from the nocodazole block, C_6-NBD-SM was transported from the rab11-positive compartments to BC. A subsequent re-internalization of the lipid analogue from the BC and transport to SAC may then have occurred, as demonstrated in figure 8f.
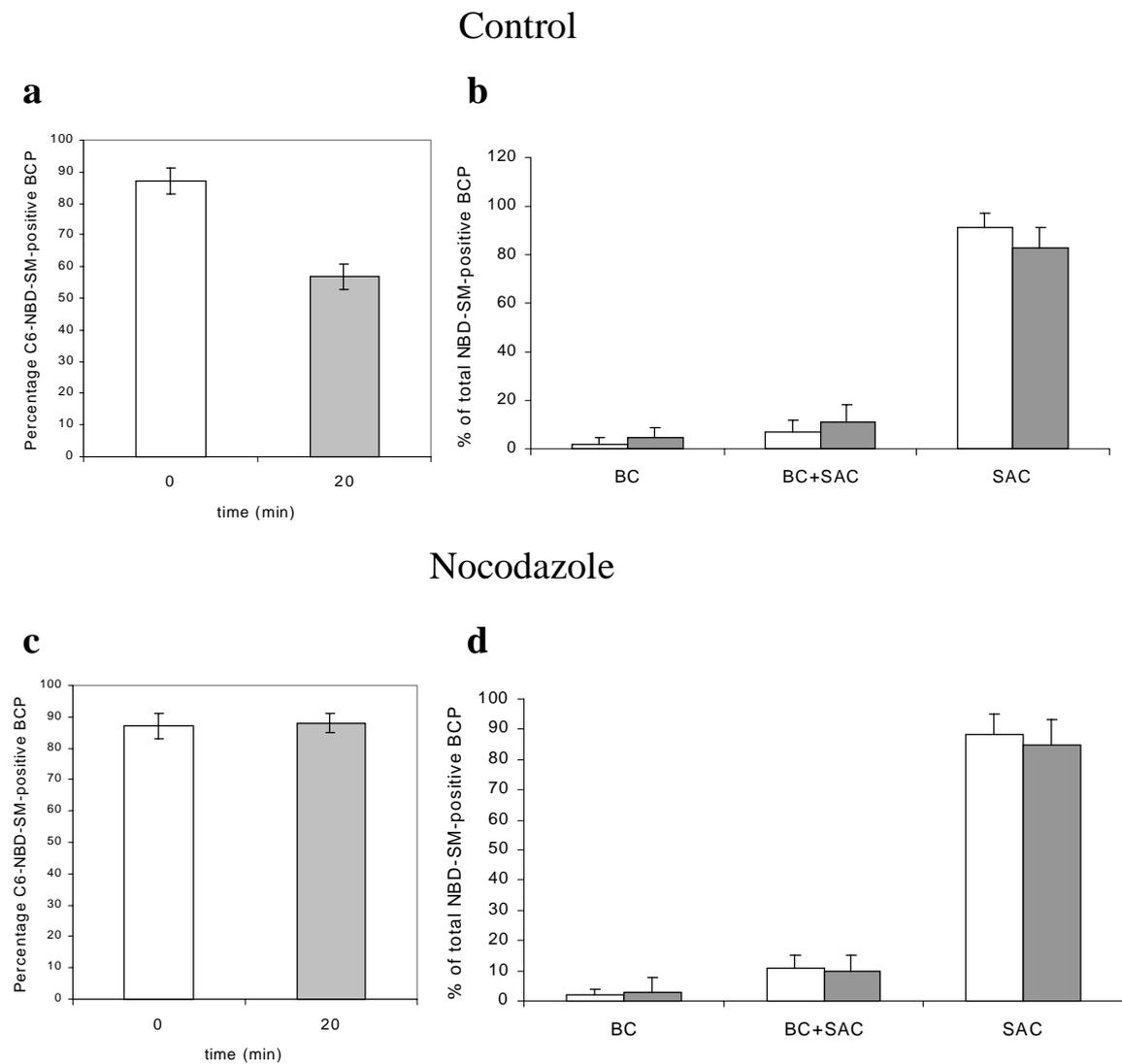
Figure 6. SAC-to-basolateral transport of C_6-NBD-SM depends on intact microtubules. The SAC was loaded with C_6-NBD-SM, as described in Materials and Methods, and the cells were treated with HBSS with or without nocodazole at 4°C for 30 min and incubated in back exchange medium, with or without nocodazole for 20 min at 37°C. Figures a and b represent the lipid distribution in control cells; c and d show the distribution in nocodazole-treated cells. In a and c, the percentage of C_6-NBD-SM-labeled BCP is shown prior and after the chase (20 min 37°C. In b and d, the distribution of the lipid analogue within the BCP is demonstrated (white bars: prior to the chase; gray bars: after the chase).
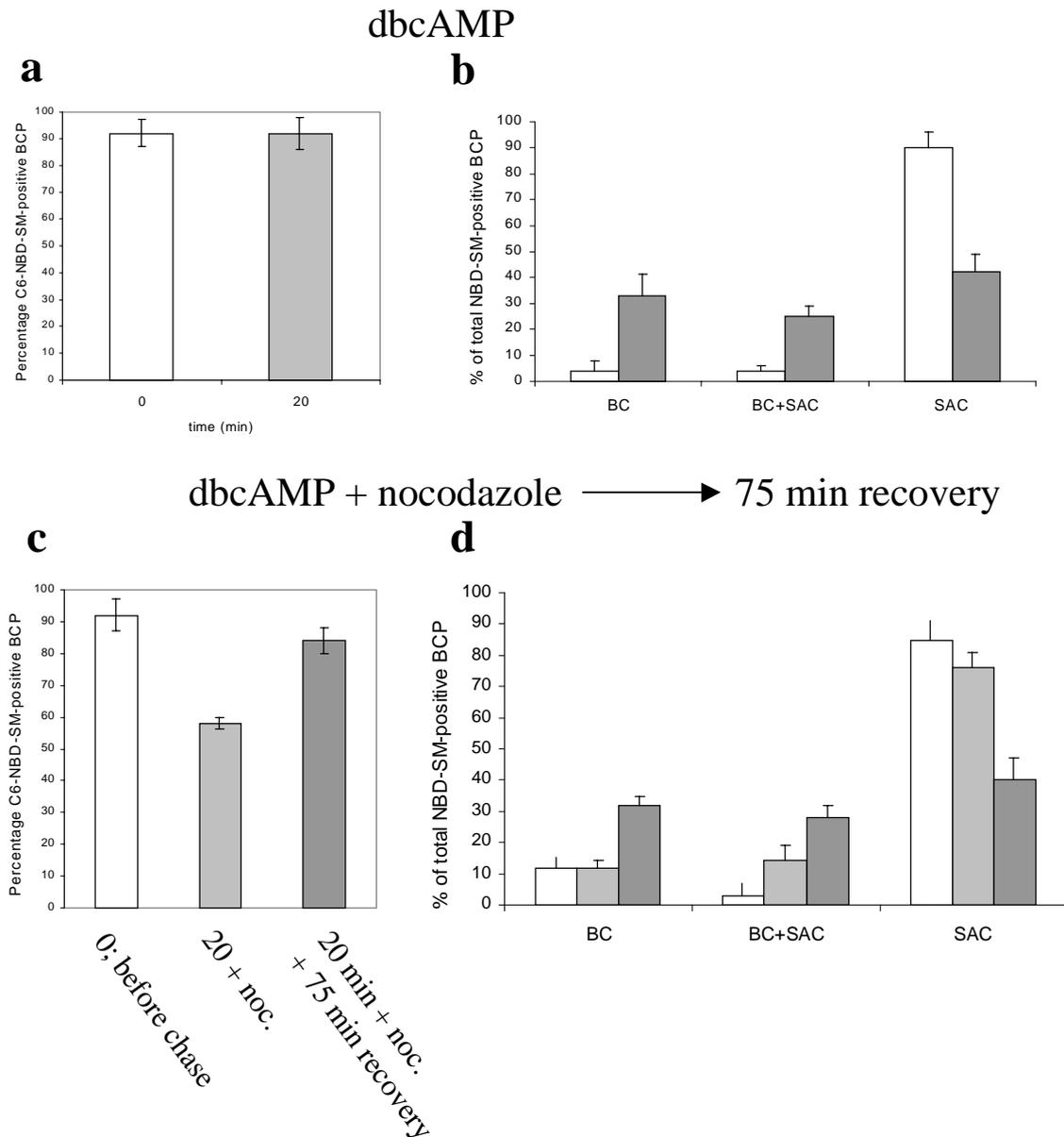
Figure 7. Nocodazole inhibits SAC-to-BC transport of C_6-NBD-SM. The SAC was loaded with C_6-NBD-SM as described in Materials and Methods. Cells were treated with HBSS with or without nocodazole and dbcAMP at 4°C for 30 min and incubated in back exchange medium, with or without the compounds for 20 min. Figures a and b represent control cells; c and d are treated cells. In a and c, the percentage of C_6-NBD-SM-labeled BCP is shown prior and after the chase (20 min 37°C). In b and d, the distribution of the lipid analogue within the BCP is given (white bars: prior to the chase; light-gray bars: after the chase). In some cases, nocodazole was removed by washing, and the cells were further incubated in back exchange medium, supplemented with dbcAMP, at 37°C for 75 min (c and d, dark-gray bars).

Figure 8. Nocodazole reversibly inhibits SAC-to-BC transport of C_6-NBD-SM in dbcAMP-treated cells. The SAC was loaded with C_6-NBD-SM as described in Materials and Methods (a, b). Cells were then treated with dbcAMP and nocodazole at 4°C for 30 min, which was followed by a chase of 20 min at 37°C in back exchange medium, supplemented with both compounds. After the chase (d), prominent labeling of the SAC is no longer apparent but the lipid is dispersed (in vesicular structures) throughout the cytosol. Cells were then washed and further incubated at 37°C for 75 min in back exchange medium lacking nocodazole. Note the reappearance of labeled SAC and BC. Asterisk represents the BC; arrows point to labeled SAC. Bar. 5μm.
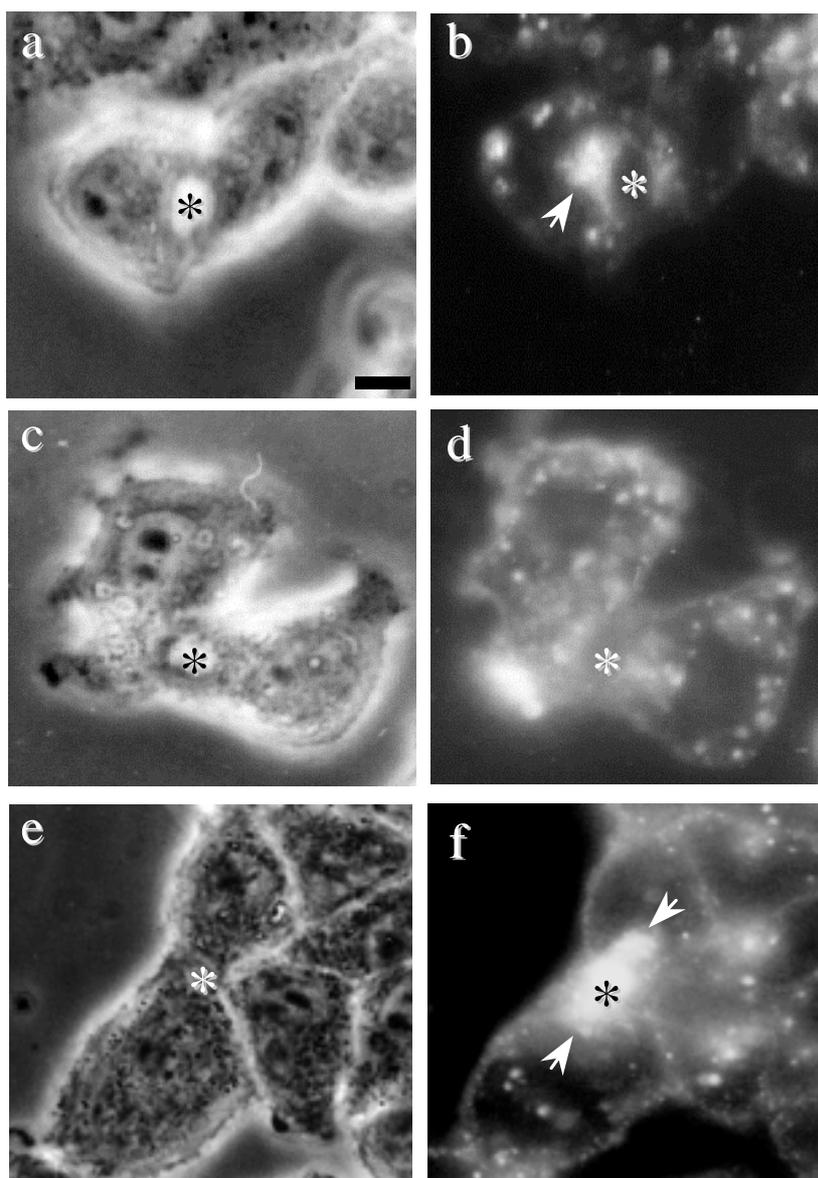
Discussion

In this study, it is demonstrated that rab11 localizes to sub-apical compartments that likely constitute a part of the apically directed transport pathways in polarized HepG2 cells. The localization of these compartments is similar to that reported in hepatocytes (Goldenring et al., 1996). Also in other epithelial cells, such as MDCK (Casanova et al., 1998) and gastric parietal cells (Calhoun and Goldenring, 1997), a sub-apical localization of rab11-containing compartments has been described. The sub-apical compartments have been shown to concentrate around the microtubule-organizing center (MTOC, Apodaca et al., 1994; Futter et al., 1998). In the endocytic pathway of nonpolarized cells, rab11 has been demonstrated to localize to the pericentriolar recycling compartments (PCRC), typically localized in the

 juxtanuclear region (Ren et al., 1998; Green et al., 1997; Ullrich et al., 1996). The sub-apical recycling compartments in polarized cells and the PCRC in nonpolarized cells have been proposed to be analogous (Apodaca et al., 1994; Zacchi et al., 1998). These compartments, likely forming a heterogeneous mixture of subcompartments, are considered to function as the sorting station, regulating delivery to specific domains at the cell surface (reviewed in van IJzendoorn and Hoekstra, 1999). Indeed, both compartments are capable of sorting PM molecules into distinct traffic pathways, which may be instrumental to serve specific PM domains. In non-epithelial cells such as fibroblasts, molecules are concentrated in the PCRC and targeted to the leading lamella upon migration of the cells (Hopkins et al., 1994). In epithelial cells, the sub-apical compartment connects the basolateral and apical membrane domains, and is believed to orchestrate the polarized targeting of proteins and lipids. Upon induction of cell polarity, the MTOC is repositioned from a juxtanuclear localization to one that faces the specialized PM domain (Houliston et al., 1987), supporting the proposed analogy between the sub-apical compartments and the PCRC. Indeed, in nonpolarized HepG2 cells, rab11 is profoundly present in the juxtanuclear area (Fig. 1c, d). Moreover, in both polarized and non-polarized HepG2 cells, rab11 colocalizes with the MTOC, identified as the site where microtubules regrow after recovery from nocodazole-treatment (Fig. 2). Our data allow for the first time a comparison of rab11 localization between the polarized and nonpolarized form of the same cells, present in a single cell culture, and strongly support the proposed analogy between the rab11-positive sub-apical recycling compartments and the PCRC.

In a previous study, we have demonstrated that C_6-NBD-SM and –GlcCer, endocytosed from the apical surface of HepG2 cells at 18°C, accumulate in a compartment located subjacent to the apical PM, i.e. SAC. In the same compartment basolaterally derived IgA, bound to the polymeric Ig receptor (pIgR) was also shown to accumulate, as indicated by a prominent colocalization of the lipids and pIgR/IgA (van IJzendoorn and Hoekstra, 1998). It was demonstrated that in the SAC, C_6-NBD-SM and –GlcCer were sorted. Thus, C_6-NBD-SM was rapidly transported from the SAC to the basolateral domain of the cells, whereas the GlcCer analogue was efficiently targeted from the SAC to the apical PM (van IJzendoorn and Hoekstra, 1998). Intriguingly, whereas the spatial organization of the rab11-positive sub-apical compartments depends on microtubules (Fig. 3), consistent with the results obtained in MDCK cells (Casanova et al., 1998), this appears not to be the case for the SAC, as identified by the accumulation of the sphingolipid analogs (Fig. 4a-d, cf. van IJzendoorn and Hoekstra, 1998). Hence, the data indicate that the SAC, where sphingolipids are sorted, are distinct from the rab11-positive sub-apical compartments and suggest that traffic in/from the sub-apical region is more complex than previously appreciated.

The complexity of trafficking from the sub-apical compartments is further emphasized by the notion that two more rab proteins, rab17 (Lutcke et al., 1993; Zacchi et al., 1998) and rab25 (Casanova et al., 1998; Calhoun and Goldenring, 1997) localize to these compartments. Since these rab proteins are expressed exclusively in epithelial cells (Lutcke et al., 1993; Goldenring et al., 1993), their involvement in polarized, i.e. apical versus basolateral,

transport is anticipated (Zacchi et al., 1998; Hunziker and Peters, 1998). Interestingly, in MDCK cells rab25 and rab11 show a considerable, although not complete degree of overlap after their dispersion with nocodazole (Casanova et al. 1998), whereas in Eph4 cells rab17-postive sub-apical compartments appeared nocodazole-inert (Zacchi et al., 1998). Although extrapolation of results obtained from different cell types should be done with caution, the available data provide support for our hypothesis that SAC likely consists of distinct subcompartments. It is tempting to suggest that polarized sorting of sphingolipids and proteins is orchestrated in the (nocodazole-inert) SAC, while the distinct rab11-containing compartments may be functionally involved in apical PM expression. The rab11-postive sub-apical compartments may thus represent an elaboration of the apical recycling system.

Elevated intracellular cAMP levels can switch the direction of polarized transport of C_6-NBD-SM from the SAC. Thus, whereas the SM analogue is rapidly transported from the SAC to the basolateral domain of HepG2 cell in control cells (Fig. 5a, b), the lipid is efficiently targeted to the apical PM after treatment of the cells with the cell permeant, non-hydrolysable dbcAMP (Fig. 7a, b). Recent results obtained in our laboratory suggest that this dbcAMP-induced rerouting is caused by PKA activation. Moreover, the pathway from the SAC to the apical PM as followed by C_6-NBD-SM and –GlcCer in dbcAMP-treated cells was found to be differentially regulated by calmodulin antagonists which suggest that distinct routes are operational between the SAC and the apical surface (van IJzendoorn and Hoekstra, submitted). Consistently, SAC-to-apical transport of C_6-NBD-SM, but not of C_6-NBD-GlcCer is dependent on intact microtubules, which thus provides an additional means to discriminate the distinct transport pathways taken by both lipids.

Surprisingly, after the chase in nocodazole-treated cells, the percentage of C_6-NBD-SM-labeled BCP decreased with ~40% (Fig. 7c), whereas that of C_6-NBD-GlcCer-labeled BCP remained constant at ~90%. Although at first sight, a decrease in percentage of labeled BCP would imply transport out of the apical pole (Fig. 6a; cf. van IJzendoorn and Hoekstra, 1998), the dependence of C_6-NBD-SM from the SAC to the basolateral domain on intact microtubules (Fig. 6c, d), renders this possibility highly unlikely. Indeed, the cellular pool of the NBD-labeled lipids did not decrease, as would have occurred when the lipid had reached the basolateral membrane, where BSA acts as a lipid scavenger (data not shown). Rather, the prominent labeling of vesicular structures throughout the cytoplasm in dbcAMP/nocodazole-treated cells (Fig. 8c) suggests that the lipid analogue was redistributed. Moreover, following recovery from the nocodazole block, the percentage of C_6-NBD-SM-labeled BCP was similarly recovered to control levels (Fig. 7c, d). Accordingly, the reestablishment of the BCP pool is related to the 'reconstitution' of a nocodazole-sensitive compartment in which the SM was located on its way from the SAC to the apical membrane. Such a compartment is likely represented by the rab11-positive compartment. Based on the available data, the following transport itinerary from the SAC to the BC is therefore proposed (schematically depicted in Fig. 9). After treatment with nocodazole and dbcAMP, C_6-NBD-SM can still be transported to the rab11-positive compartments, in spite of being dispersed and, importantly, implying that this transport step is microtubule-independent. The remaining percentage of labeled BCP is

accounted for by nocodazole-inert SAC-associated C_6-NBD-SM that has not yet been transported to the rab11-postive structures. Following recovery from the nocodazole block, the lipid is then transported from the rab11-positive compartments, to which we will refer as sub-apical intermediate compartments (SIC), to the BC. From the BC, a fraction of the C_6-NBD-SM is then likely transported again to the nocodazole-inert SAC, thus entering an apical recycling pathway in the presence of dbcAMP and a basolateral pathway in its absence. Interestingly, the SIC appears to be accessible for SAC-derived, but not BC-derived SM. Indeed, apical internalization of sphingolipids is microtubule-independent, in contrast to subsequent delivery to the nocodazole-inert SAC (van IJzendoorn and Hoekstra, 1998). Hence, it is suggested that the SIC functions as an intermediate compartment in the SAC-to-apical transport route of SM in dbcAMP-treated cells.
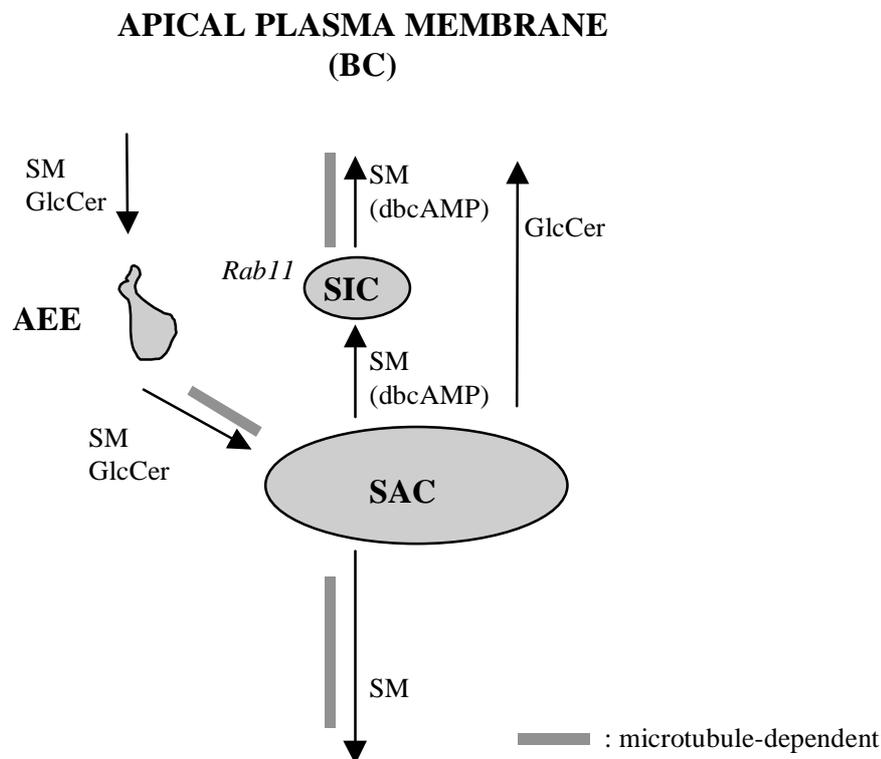

Figure 9. Schematic representation of sphingolipid trafficking from the SAC to the apical PM and the involvement of the SIC in HepG2 cells. SM and GlcCer are endocytosed from the apical PM and transported, presumably via apical early endosomes (van IJzendoorn and Hoekstra, 1998) to the SAC. From the SAC, GlcCer is efficiently recycled back to the apical membrane, whereas SM is transported to the basolateral membrane. However, when cells have been treated with dbcAMP, SM is rerouted into an apical PM-directed pathway. This route, in contrast to that of GlcCer, includes trafficking via rab11-positive sub-apical intermediate compartments (SIC). Moreover, whereas exit of both lipids, bound for the apical PM, from the SAC is microtubule-independent, final apical delivery of SM, but not of GlcCer, is microtubule dependent.

According to this model, transport from the SAC to the SIC and from the SIC to the BC is not critically dependent on the intact spatial organization of the SIC. This is inferred from the observation that the transport cycle between the nocodazole-inert SAC and the BC seems fully restored after 75 min, whereas the spatial 'reconstitution' of the rab11-postive SIC has not (Fig. 3). In addition, transport of C_6-NBD-SM from the SIC to BC is dependent on intact microtubules, while transport of C_6-NBD-SM from the nocodazole-inert SAC to the basolateral domain of non-dibutyryl cAMP-treated cells also depends on intact microtubules. These data suggest that the involvement of microtubules in vesicle-based transport and in the structural organization of transport intermediates is not strictly related.

Our data suggest that the trafficking of C_6-NBD-GlcCer from the SAC to the BC bypasses the SIC, suggesting that the SIC is involved in selective transport from the SAC to the apical surface. Possibly, such selective transport reflects a process of signal-mediated apical delivery. Interestingly, rab11 has been shown to colocalize with the H^+/K^+-ATPase in sub-apical tubulovesicular compartments (Goldenring et al. 1996), and the translocation of the H^+/K^+-ATPase from a sub-apical endosomal compartment to the apical surface in epithelial cells is enhanced when cAMP levels are elevated (Forte and Yao, 1996). These observations combined with our data on signal-induced targeting of SM from the SAC into a specific apical surface-directed pathway, support the hypothesis of a rab11-positive SIC-mediated traffic route that is employed for regulated, selective expression of PM molecules at the apical surface.